Available online at www.sciencedirect.com
ScienceDirect
C. R. Mecanique 337 (2009) 562–572
COMPTES RENDUS MECANIQUE

Combustion for aerospace propulsion

Full coverage film cooling using compound angle

Brice Michel [a,*], Pierre Gajan [a], Alain Strzelecki [a], Nicolas Savary [b], Azeddine Kourta [c], Henri-Claude Boisson [c]

[a] *ONERA/DMAE, 2, avenue Edouard-Belin, 31055 Toulouse cedex, France*
[b] *Turbomeca, avenue Joseph-Szydlowski, 64511 Bordes cedex, France*
[c] *IMFT, UMR 5502 CNRS/INPT/UPS, avenue du Prof. Camille-Soula, 31400 Toulouse, France*

Available online 17 July 2009

Abstract

An experimental and numerical study is carried out on a cooling film issuing from a multiperforated wall of a simplified combustor. The objectives of this work are to achieve a better understanding of the dynamics of the film and to construct an experimental database on a simplified geometry in order to test numerical models. A parametric study of film cooling efficiency based on the direction of the cooling air injection is presented and shows that a swirling injection greatly enhances the cooling efficiency. As accounting for multiperforated walls in numerical simulations cannot be done at the jets scale because of computing resources, in this article are presented RANS computations performed using a uniform boundary condition to provide the injection of coolant. Two injection models are applied on this boundary and numerical results are compared to experimental data in the recovery region. The standard model is shown to be totally inappropriate while the multiperforation model delivers promising results although some weaknesses appear very close to the wall. ***To cite this article: B. Michel et al., C. R. Mecanique 337 (2009).***

Résumé

Refroidissement par multiperforation utilisant des orifices inclinés transversalement. Une étude expérimentale et numérique est menée sur un film de refroidissement provenant d'une paroi multiperforée d'une chambre de combustion simplifiée. Les objectifs de ce travail visent à améliorer la compréhension de la dynamique du film et à construire une base de données expérimentales afin de pouvoir tester des modèles numériques. Une étude paramétrique de l'éfficacité du refroidissement par film basée sur la direction de l'injection de l'air de refroidissement est présentée et montre que la mise en giration du film améliore significativement l'efficacité du refroidissement. La prise en compte des parois multiperforées à l'échelle de jets s'avérant très difficile dans les simulations numériques à cause des ressources informatiques nécessitées, dans ce papier sont présentés des calculs RANS réalisés avec une condition limite uniforme utilisée pour assurer l'injection de l'air de refroidissement. Deux modèles d'injection sont appliqués sur cette condition limite et les résultats numériques sont comparés aux données expérimentales dans la zone de recouvrement. Le modèle standard s'avère totalement inapproprié tandis que le modèle Multiperforation montre des résultats encourageants même si des faiblesses apparaissent en proximité de la paroi.***Pour citer cet article : B. Michel et al., C. R. Mecanique 337 (2009).***

Keywords: Combustion; Combustors; Effusion cooling; Jets in cross flow; Mixing

* Corresponding author.
E-mail addresses: brice.paul.michel@gmail.com (B. Michel), pierre.gajan@onecert.fr (P. Gajan).

1631-0721/$ – see front matter
doi:10.1016/j.crme.2009.06.012

Mots-clés : Combustion ; Chambre de combustion ; Refroidissement par multiperforation ; Jets transverses ; Mélange

1. Introduction

Over the last decades, aeroengine internal cooling has become a crucial issue. Indeed, to reduce polluting emissions, new lean injectors are requiring a higher amount of primary air and thus less air is available for cooling. Besides, to improve the thermodynamic cycle efficiency, the temperature of this air coming from the compressor exit has been doubled in 30 years of engine development, increasing again the difficulty to provide a proper thermal protection. To reach the latter, an efficient method called Full Coverage Film Cooling (FCFC) is currently used in aeroengines to protect and increase the lifetime of parts exposed to high temperatures. In this approach, fresh air coming from the casing goes through a multiperforated liner and enters the combustion chamber. The associated micro-jets coalesce and produce a film that protects the internal wall face from the hot gases (Mayle and Camarata [1], Rouvreau [2]). As new combustion chamber development requires CFD computations, sub-millimeter holes must be taken into account. However, their number is far too large to allow a complete description. A specific modelling is required and this modelling must be validated experimentally. Crawford et al. [3] carried out a FCFC heat transfer study with normal, 30 deg slant and 30 deg $\times$ 45 deg compound-angled holes. They found that the compound-angled injection is the preferable one. To take advantage of this conclusion, a cylindrical liner is investigated in this article. Cooling air is injected with a compound angle inducing a rotating motion of the cooling film. The recovery region is investigated experimentally to provide flow visualizations using PLIF and a velocity and concentration database. Although many studies investigated thermal performances (Schmidt et al. [4], Ligrani et al. [5]) or dynamics (Gustafsson [6], Miron et al. [7]) of the cooling film, there are few concentration data. Previously, the PLIF technique was however used by Rouvreau [2] on a multiperforated plate. He observed the evolution of the film along 21 rows of holes and concluded that a steady state is obtained at the 8th row. However, the effect of the compound angle was not investigated as holes were only 30 deg slant. Both the multijets injection area and the recovery region are computed. A boundary condition is proposed to model the multiperforated liner. Objectives are to identify the effect of compound angle and to test the multihole injection model accuracy.

2. Experimental facility and instrumentation

2.1. Experimental setup

A special wind tunnel working at ambient temperature was built to investigate aerodynamically the film cooling issuing from a multiperforated ring as an application of combustor walls cooling techniques. As shown in Fig. 1, ambient air passes through the convergent intake and enters a three meter long pipe, 100 millimeters in diameter, to form the fully developed primary flow. Secondary flow is provided using a 70 bar tank and a sonic nozzle measure the mass flow rate with accuracy better than 1%. This secondary flow arrives in a tranquilization chamber through four entrances before penetrating into the main flow through the multiperforated ring to form the cooling film. The 100 mm internal diameter (D) glass tube and the lateral windows are made of Suprasil glass in order to permit UV lighting for PLIF measurements. The total mass flow rate is then measured by a turbine flow meter with an accuracy better than 0.5%.

In this study, the multiperforated combustor liner is modelled by a 100 mm internal diameter ring which is provided by Turbomeca to ensure a good representation of actual multiperforated walls. Injection holes, drilled by laser impulsions, have a compound angle orientation, described in Fig. 2: angle β is in the plane $\langle e_\theta, e_x\rangle$ whereas angle α is in the plane $\langle e_x, e_r\rangle$ when $\beta = 0°$ and in the plane $\langle e_r, e_\theta\rangle$ when $\beta = 90°$. Two multiperforated rings are used: one with $\beta = 0°$ and another one with $\beta = 90°$, further referred to as "Axial ring" and "Swirling ring" respectively. Angle α has a fixed value of 30°. Holes pattern is a staggered array of 9 rows with 99 holes each.

2.2. Experimental techniques

During these experiments, two experimental techniques were applied. In a first step a 2D LDA system was used in order to obtain a detailed description of averaged velocity and turbulence field in six pipe sections located upstream

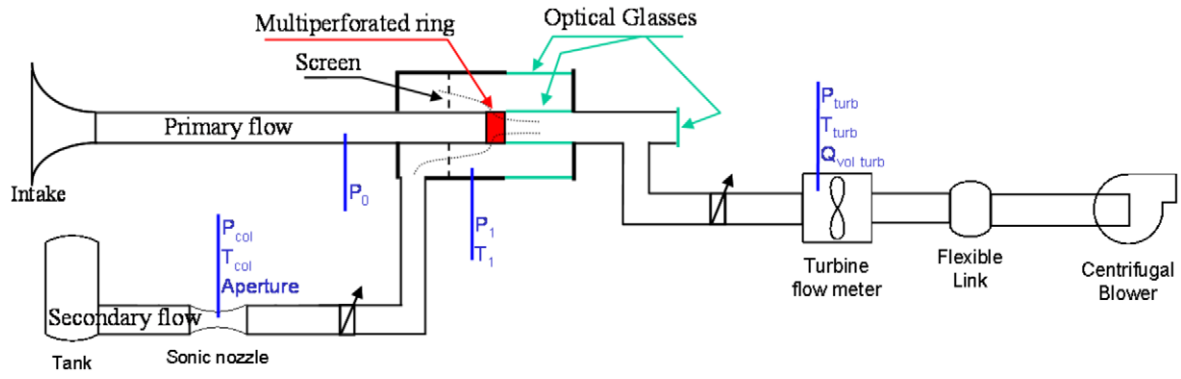

Fig. 1. Experimental setup.

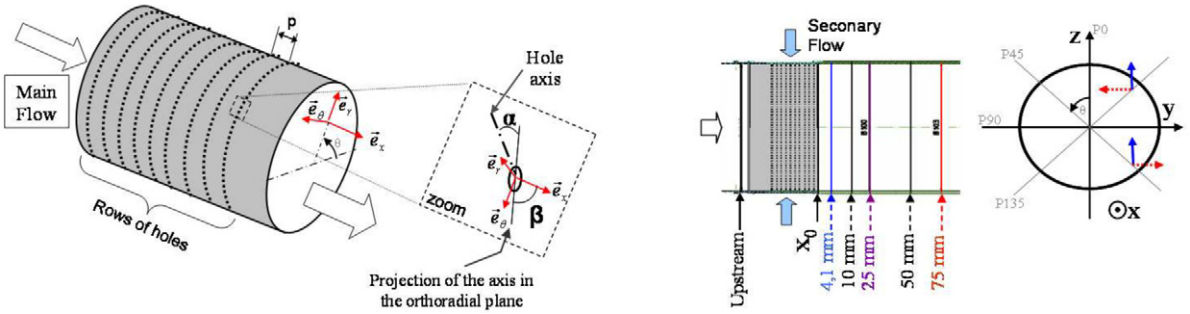

Fig. 2. Multiperforated ring and measurement positions.

and downstream of the multiperforated ring (4.1, 10, 25, 50 and 75 mm). The size of the measurement volume is equal to 1.3 mm in length and 90 μm in diameter. The flow is seeded with droplets of olive oil. Measurements are performed on 6 positions shown in Fig. 2. In order to determine the three velocity components we assume that the flow is axisymmetric and, by comparing the measurements obtained on two orthogonal radiuses, the velocity and turbulence field can be determined.

The PLIF technique is used to study the mixing of the film cooling with the primary flow. As the Schmidt number is close to one in our experiments, concentration structures observed on instantaneous fields are a good representation of velocity structures. Two types of measurement are taken: cross view and longitudinal view. The transverse flow is analyzed in different pipe sections downstream of the jet exits (4.1, 10, 50 and 75 mm). The laser sheet is orthogonal to the pipe axis and the camera is placed in front of the open section of the pipe. For longitudinal views, the respective positions of the laser sheet and the camera are permutated. The PLIF technique uses a monochromatic light source which is formed into a sheet and passed through the flow field. The light source excites an energy transition in a marker species, which fluoresces upon relaxation [8]. The fluorescence is captured on an imaging array. In this study, acetone vapor is used as a tracer. Acetone fluorescence is a linear function of both incident laser energy and acetone concentration. Acetone absorbs in UV light (225–320 nm; 278 nm peak) and emits in the visible spectrum (350–550 nm, 435 peak) allowing for the use of CCD arrays. A quadrupled Nd YAG Spectra Physics laser provides a 90 mJ, 266 nm pulse which is formed into a sheet and focused to a waist in the test section. The sheet thickness is 0.3 mm in the measured flow field regions. Two lens arrangements are used to form either a parallel or a diverging laser sheet. The acetone vapor is obtained by bubbling filtered air through two pressurized cylinders. A 1280 × 1024 pixel CCD camera captures the fluorescence. The incoming light is first amplified by an intensifier. For each test, 1000 images are recorded. Auxiliary measurements are performed without flow rates to obtain the concentration values: the measuring volume is insulated and a known acetone mass is introduced. As the laser enters the measurement volume, acetone absorbs the incident light and then the fluorescence decrease along the laser sheet. Besides, the light distribution in the laser sheet is not uniform because of the optical apparatus. It is therefore necessary to account for these phenomena to get proper results. Post-processing is then applied to eliminate the background, scale measurements, correct light

absorption and light distribution. Finally, concentration is normalized by the initial concentration of the secondary flow C_0.

2.3. Aerodynamic flow parameters

A review of the large number of parameters influencing the film efficiency is given by Bogard and Thole [9]. In film cooling, the main aerodynamics parameters are blowing ratio M and momentum flux ratio I defined in Eqs. (1) and (2) respectively,

$$M = \frac{\rho_{jet} V_{jet}}{\rho_0 V_0} \tag{1}$$

$$I = \frac{\rho_{jet} V_{jet}^2}{\rho_0 V_0^2} \tag{2}$$

where V is the bulk velocity. The blowing ratio scales the thermal transport capacity since the convective transport is proportional to $C_p \rho V_{jet}$. The momentum flux ratio scales the dynamics of the interaction of the mainstream with the exiting coolant jet as the mainstream impact pressure causes the coolant jet to turn toward the wall. Rouvreau [2] investigated a full coverage film cooling area and clearly demonstrated that these two parameters are independent, but have the same kind of effect on velocity profiles. In our study, both primary flow and secondary flow are at ambient temperature and hence, blowing ratio and momentum flux ratio are not independent any more. Primary flow is supposed to represent burned gases and secondary flow is supposed to represent the cold air coming from the compressor. In our case an M ratio of 8.8, corresponding to values considered in combustors, was used. Finally, in order to simulate real flows inside combustors, Reynolds similarity was also respected. Reynolds number is based on main stream bulk velocity and pipe radius and is valued at 17 700. The Reynolds number in the hole is 1200. It is not the value encountered in real combustors but, due to temperature differences, all non-dimensional parameters cannot be reached.

3. Influence of the compound angle

In this section, experimental results obtained for both axial and swirling injections are compared to analyse the effect of the compound angle. On each graph, axial or swirling injection results are reported on the negative or positive radius respectively.

3.1. Mean velocities

Mean velocity profiles measured upstream and downstream of the injection zone are plotted on Figs. 3 and 4. Considering that the blowing ratio is 8.8 the air injected through the wall drives the main stream. Consequently, changing the injection hole orientation leads to change the driving process orientation. For this reason the longitudinal velocity component reported on Fig. 3a is reduced at the pipe center in the case of axial injection whereas, with compound injection, the main stream is driven in a swirling motion, as it is clearly shown in Fig. 4b. The rotation induces a blockage process resulting in an increase of lengthwise velocity in the central zone of the pipe (Fig. 3b). Between both configurations, longitudinal velocity profiles are therefore strongly different.

In order to estimate the film thickness using a velocity criterion, longitudinal component reduced by velocity at the pipe center is plotted on Fig. 4a for axial injection and tangential component is plotted on Fig. 4b for compound injection. Film thicknesses are determined when downstream profiles reach the upstream profile with a discrepancy less than 0.05 m/s. The thickness obtained with the axial injection is half the one measured with the swirling injection (from 0.07 to 0.12 compared to 0.2 r/D). Another important result is the behaviour of the film in the streamwise direction: with axial injection, the film is getting thicker with the streamwise distance while the thickness remains nearly constant in the case of swirling injection. This result suggests that the film establishes in a much shorter distance in the latter case.

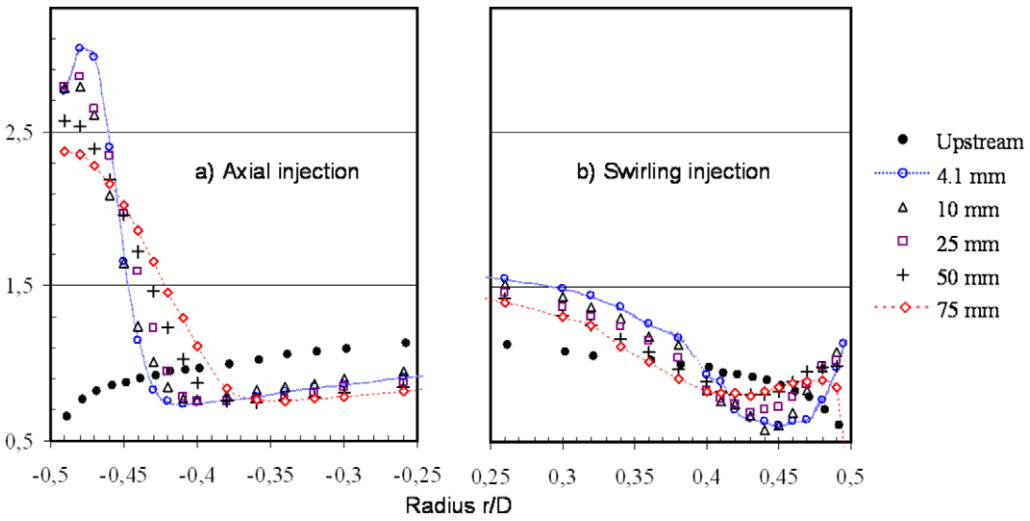

Fig. 3. Comparison of longitudinal velocity profiles (V_x / V_0) measured for axial (left) and swirl (right) configurations.

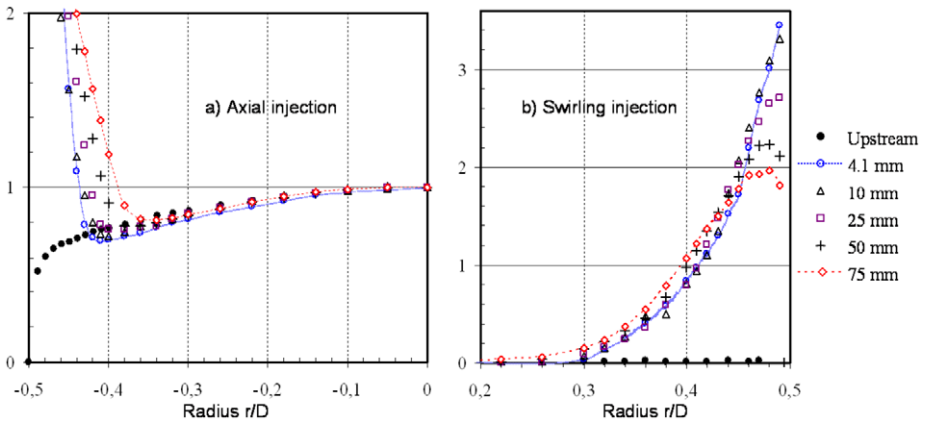

Fig. 4. Zoom in longitudinal velocity profiles reduced by velocity at pipe center for axial injection ($V_{x,r} / V_{x,0}$, left) and tangential velocity profiles for swirling injection (V_t / V_0, right).

3.2. Turbulence

Turbulence intensity profiles reported on Fig. 5a confirm the previous results on the film thickness and also indicate that a compound injection increases turbulence intensities by 5 to 10 percent compared to an axial injection. Measurements of turbulent time scales are performed with one million acquisition points and, using the Taylor hypothesis, turbulent length scales are calculated. This hypothesis assumes a frozen turbulence and is applicable in the case of small turbulence circulations so that the advection of a turbulent field can be taken to be entirely due to the mean flow. While this hypothesis is likely to be validated upstream the wall injection, it is not the case in the cooling film because of the high levels of turbulence. Nevertheless, results reported on Fig. 5b can be interpreted as a good estimate of the length scale behaviours as the significance of the results is justified by the matching of the length scale values in the film in the swirling case with the injection hole size, and also by the matching of downstream injection profiles with the upstream profile at the pipe center. Behaviours of length scales in the cooling film generated by each configuration are very different in the region close to the wall: a constant value of L/D about 0.06 is found for the axial film while in the swirling film configuration the turbulence scales increase continuously from 0.008 to 0.04 when moving away from the dilution zone (from 4.1 mm to 75 mm). These length scales can be linked to the instantaneous structures observed with PLIF (Fig. 7).

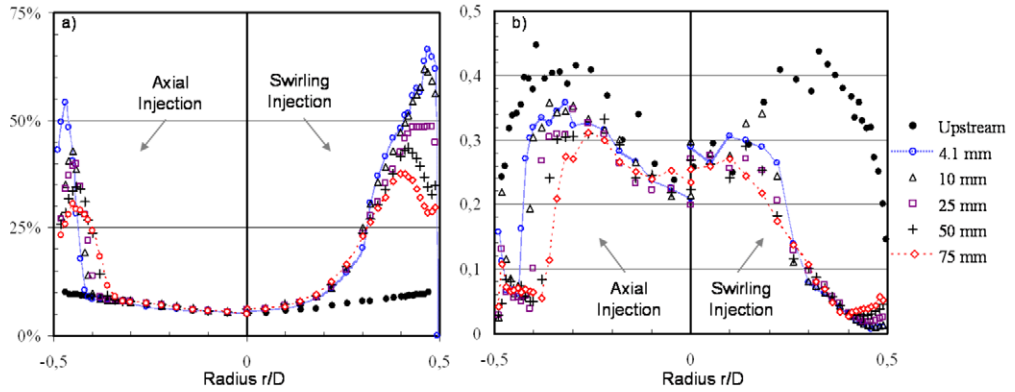

Fig. 5. Comparison of turbulence intensities ($\sqrt{k}/V_0$, left) and turbulence scales (Lxx/D, right).

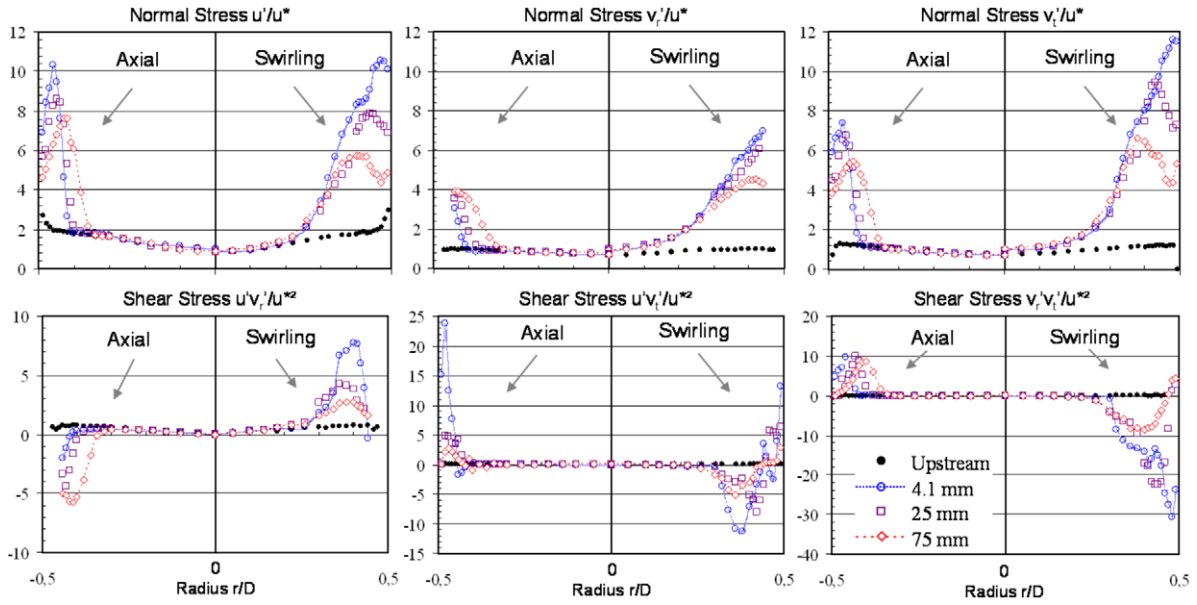

Fig. 6. Comparison of normal stresses $\sqrt{\overline{u_i'u_i'}}/u^*$ and shear stresses $\overline{u_i'u_j'}/u^{*2}$.

In order to understand mechanisms of turbulence production, normal and shear stress profiles are plotted on Fig. 6. Turbulence resulting from the interaction of the cooling film and the main stream is anisotropic in both axial and swirling configurations. Nevertheless, with swirling injection, the induced rotation provokes important gradients in the radial direction. These additional gradients increase normal stresses in the radial and the tangential directions, as it is clearly shown in Fig. 6. These increases lead to a more isotropic turbulence in the case of swirling injection.

Shear stresses profiles plotted on Fig. 6 show strongly different behaviour between the axial case and the swirling case. The Boussinesq assumption can be discussed by comparing shear stresses to mean velocity profiles of Figs. 3 and 4. The general formula can be adapted to our configuration in the recovery region: first, the stresses are rewritten in cylindrical coordinates, then a rotation invariance is considered due to the axisymmetry of the mean flow, and radial gradients are eventually neglected as they are very low. These considerations lead to the following equations:

$$\overline{u'v_r'} = -\nu_t\left(\frac{\partial \bar{U}}{\partial r}\right) \tag{3}$$

$$\overline{u'v_t'} = -\nu_t\left(\frac{\partial \bar{V}_t}{\partial x}\right) \tag{4}$$

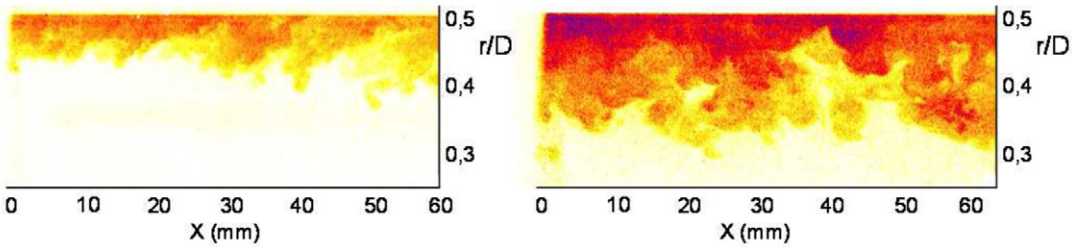

Fig. 7. Instantaneous concentration fields with axial (left) and swirling (right) injection.

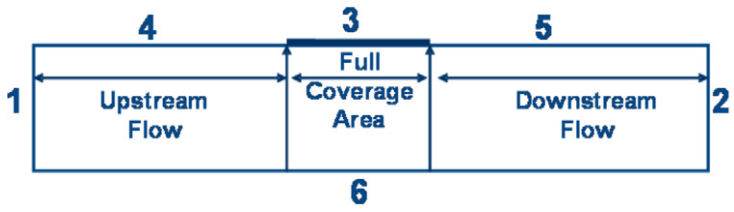

Fig. 8. 2D computational domain (9753 nodes).

$$\overline{v_r' v_t'} = -\nu_t \left(\frac{\partial \bar{V}_t}{\partial r} \right) \tag{5}$$

The longitudinal velocity profiles point out a strong positive gradient with the axial injection or a negative one and then, closer to the wall, positive one, with the swirling injection. As the shear stress $\overline{u' v_r'}$ shows opposite signs, the Boussinesq assumption is qualitatively verified for this stress. Reasoning the same way on other shear stresses, the assumption appears to be qualitatively validated in the case of swirling injection. On the other hand, with axial injection, the Boussinesq assumption is not verified for the shear stresses $\overline{u' v_t'}$ and $\overline{v_r' v_t'}$ as mean tangential velocities measured experimentally are null on reaching the first downstream position. In fact, these shear stresses are a consequence of local structures generated by the micro jets. However, at the measuring positions, as there is no memory effect with such modelling, $\overline{u' v_t'}$ and $\overline{v_r' v_t'}$ shear stresses are only linked to mean velocity gradients, which are null. The Boussinesq assumption being the basis of RANS modelling, its validity have an impact on numerical simulations.

3.3. Concentration

Concentration fields in a longitudinal plane are given in Fig. 7 for both axial and swirling injections. It is important to notice that the film remains attached to the wall ($r/D = 0.5$) thus providing a good wall protection. Instantaneous pictures show coherent structures that develop in the shear layer between the cooling film and the main stream.

Mean concentration profiles obtained with the PILF technique are presented in Fig. 12 for both configurations. They indicate slightly higher levels at the wall and a film twice thicker in the case of swirling injection. To ensure the mass conservation of acetone, the lower axial velocity of the swirling injection must be considered. Following the mass transfer analogy to heat transfer of Shadid and Eckert [10], the concentration field can be interpreted as a good estimation of the adiabatic effectiveness of the film cooling. Consequently, Fig. 12 shows that the protective layer is greatly enhanced with the swirling injection.

4. Numerical modeling

Computations of this experiment are performed using RANS modelling on a 2D axisymmetric domain shown in Fig. 8. Turbulence is taken into account by the standard *k-epsilon* model. At the inlet (face 1), measured LDA velocity and turbulent kinetic energy profiles are imposed as boundary conditions. On the exit plane (face 2), the ambient static pressure is imposed. A wall law is used on faces 4 and 5. Boundary condition 6 is the axis of symmetry of the mesh. As the number of sub-millimeter holes is far too large to allow a complete description, coarse grids are usually used in combustor calculations, and air from effusion cooled walls is injected with a uniform boundary condition. In this study

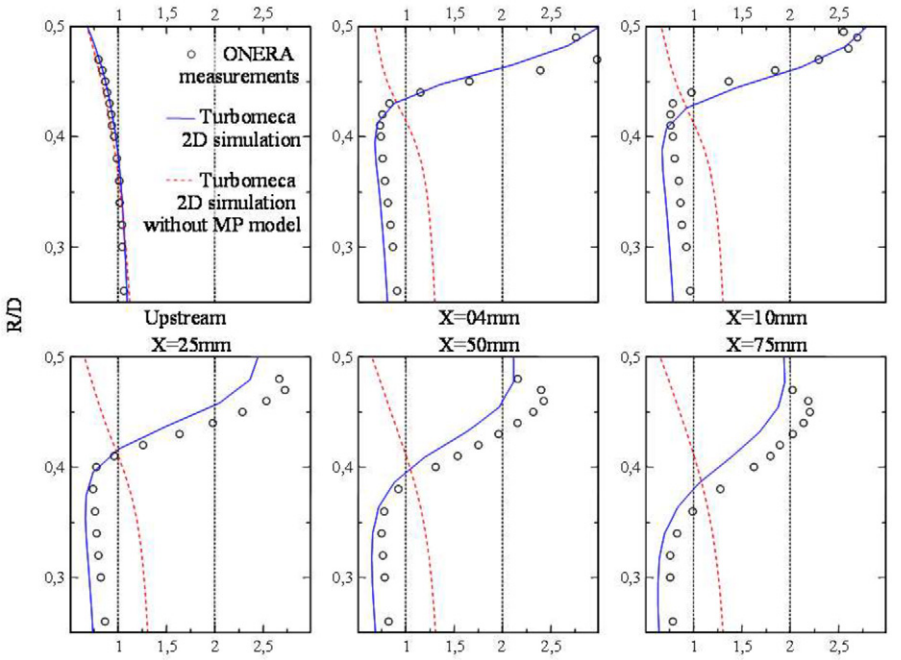

Fig. 9. Mean velocity profiles (U/U_0) of the axial configuration.

a coarse mesh has been used and the 2D axisymmetric mesh necessitates that the multiperforation zone is represented by a uniform boundary condition imposed on face 3. These simulations have been performed in axial and swirling effusion cooling configuration. In the case of effusion cooling, streamwise momentum flux of the jets has to be reached to ensure a proper description of the cooling film [11]. To provide the injection of coolant on the uniform boundary, the MultiPerforation Model (MP Model) is used. In this model, a correction is applied on the coolant velocities to provide the correct mass (M, Eq. (1)) and momentum (I, Eq. (2)) fluxes entering into the combustor. A description of the MultiPerforation Model is given by Mendez and Nicoud [11]. The main advantage of this method is that it is not necessary to mesh every sub-millimeter hole, and thus it allows the use of coarse grids and even axisymmetric simulations. In order to quantify the benefits of such a MP Model, the 2D simulations have been performed with a standard injection model through the whole boundary condition. With a standard injection model, the boundary velocity is reduced to provide the correct mass flux but there is no momentum correction. The results of these datum simulations are shown only on the velocity profiles figures.

4.1. Prediction of axial injection

In the case of axial injection, the cooling film induces a high speed layer on the longitudinal velocity component which is qualitatively described by the numerical simulations using the MP model, as shown in Fig. 9. The simulation without the MP model gives entirely wrong results compared to experiments. Despite the good agreement between MP model and measurements, some discrepancies can be observed. The film thickness is well predicted by the simulation in planes $X = 4$ mm and $X = 10$ mm but the film dynamics is under-predicted in downstream planes. This may be caused by the k-epsilon model which assumes a homogeneous and isotropic turbulence which, in that case of the shear layer, is far from being verified. Thus a too important diffusion may dissipate artificially the cooling film.

As a confirmation of previous remarks about the film dissipation, turbulent energy profiles obtained by RANS computations (shown in Fig. 10) do not reproduce correctly the experimental profiles. In the case of axial injection, the turbulent layer is overestimated resulting in a too fast dissipation of the film.

As discussed in Section 3.2, the turbulence is more isotropic and in better agreement with the Boussinesq assumption in the case of swirling injection. These hypotheses being the basis of RANS modelling, a better agreement with the experiment is found on downstream positions ($X = 25$ and $X = 50$ mm) for the swirling case.

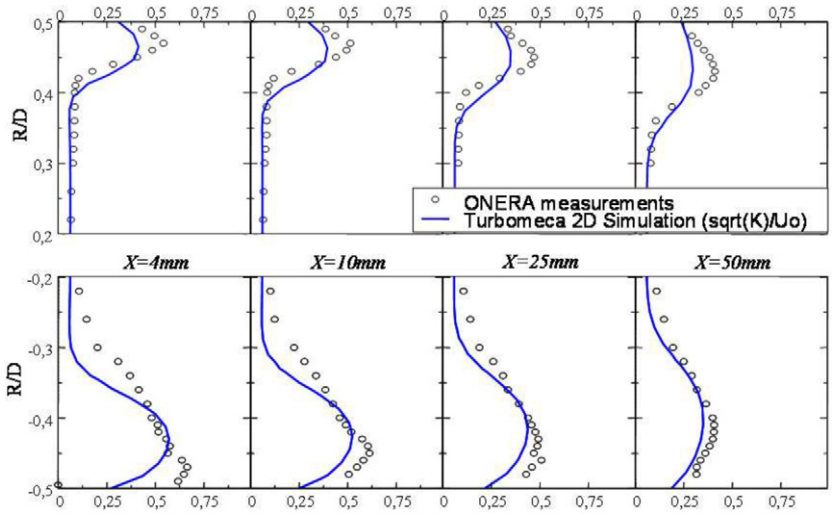

Fig. 10. Turbulent intensity profiles obtained with MP model in the axial (top) and swirling (bottom) configurations.

4.2. Prediction of swirling injection

With swirling injection, axial and tangential velocity profiles (Fig. 11) are in much better agreement with the experiments than in the axial injection case. This is due to the structure of the flow: in the swirling injection case, the cooling air injected through the effusion holes forms a thick and coherent swirling film that is convected downstream of the effusion holes. In that case, the velocity gradients at the wall are much lower than in the axial injection case. The two equation turbulence model used is based on an isotropic hypothesis and consequently the diffusion of the calculated cooling film is in better agreement with experiments in the swirling configuration. In that case, the simulations which does not use a MP model predicts wrong velocity results, especially considering the tangential velocity which is quasi inexistent in the simulation without momentum correction. As in the axial configuration, despite the good agreement between MP model simulation and measurements, the simulation cannot predict the acceleration of the flow in the near wall region. This acceleration is the result of the axial entrainment of the swirling flow resulting in a helical cooling film. This entrainment is not predicted by the simulation because it is generated by hole/flow interactions that the uniform boundary condition used to represent effusion cooling cannot predict.

Like the mean velocity profiles and the turbulence profiles, the concentrations profiles of effusion air downstream the multiperforated plate (see Fig. 12) are well reproduced by the simulations except in the near wall region. These good results confirm that this kind of simulation using MP model boundary conditions are well adapted to prediction of the flow dynamics and mixing in swirling effusion cooled combustors.

5. Conclusion

A valuable database has been elaborated on a simplified multiperforated combustor. It is shown that the compound angle has a strong effect on the dynamics of the flow, resulting in a rotation of the cooling film which keeps attached to the wall and induces an intensive turbulence. Comparison to axial injection shows that film thickness and turbulence are greatly increased with compound angled holes. Numerical simulations are performed using a uniform boundary condition to provide the injection of coolant. Applied on this boundary, the standard injection model is shown to be not adapted to these configurations. On the contrary, this paper demonstrates that the MP model can be a powerful tool for the simulation of the complex flow developing into strongly multiperforated combustors. Main features of this flow are predicted by numerical simulations using the MP model. In the vicinity of the wall, however, discrepancies occur. In this zone, the behaviour of the flow is important when dealing with wall fluxes. The next stage of this work will be devoted to enhancement and further validation of this type of models.

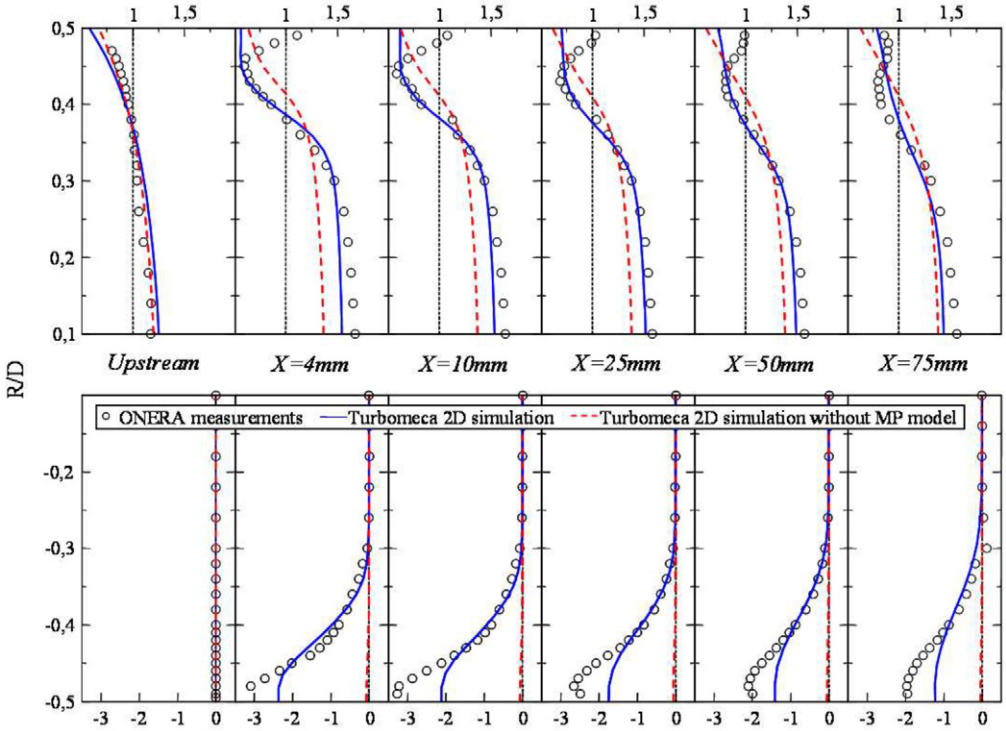

Fig. 11. Mean longitudinal (top) and tangential (bottom) velocity profiles in the swirling configuration.

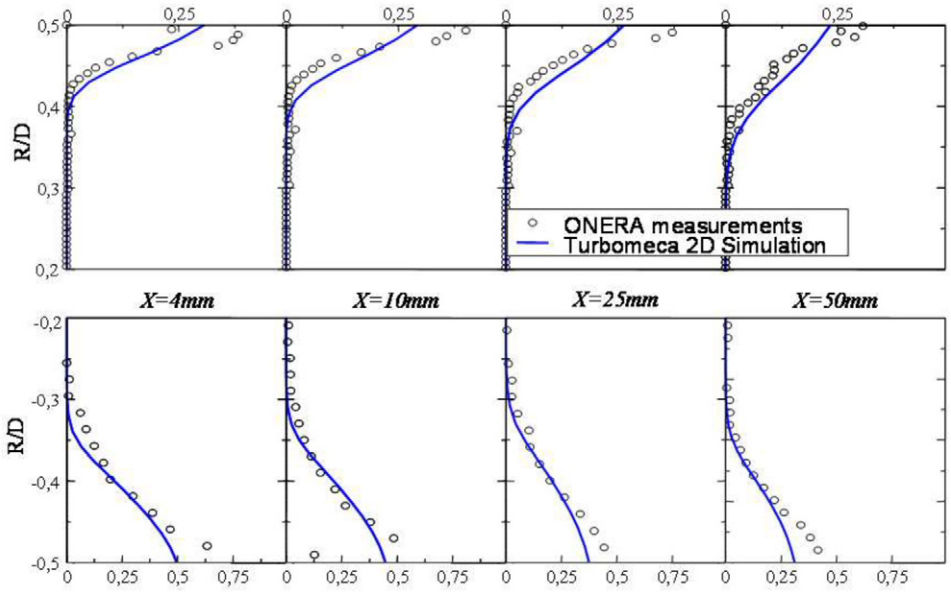

Fig. 12. Concentration profiles in axial (top) and swirl (bottom) configurations.

Acknowledgements

This work takes part of the EGISTHE program (Études générales innovantes sur les turbines hautement economiques) funded by the French Government through the Délégation générale pour l'armement.

References

[1] R.E. Mayle, F.J. Camarata, Multihole cooling effectiveness and heat transfer, Journal of Heat Transfer 97 (4) (Nov. 1995) 534–538.
[2] S. Rouvreau, Etude expérimentale de la structure moyenne et instantanée d'un film produit par une zone multiperforée sur une paroi plane, Application au refroidissement des chambres de combustion des moteurs aéronautiques, Ph.D. thesis of Poitiers University, France, 2001.
[3] M.E. Crawford, W.M. Kays, R.J. Moffat, Full-coverage film cooling. Part I: Comparison of heat transfer data for three injection angles, Journal of Engineering for Power 102 (Oct. 1980) 1000–1005.
[4] D.L. Schmidt, B. Sen, D.G. Bogard, Film cooling with compound angle holes: heat transfer and adiabatic effectiveness, Journal of Turbomachinery 118 (Oct. 1996) 807–813.
[5] P.M. Ligrani, A.E. Ramsey, Film-cooling from spanwise-oriented holes in two staggered rows, Journal of Turbomachinery 119 (1997) 562–567.
[6] B. Gustafsson, Experimental studies of effusion cooling, Ph.D. thesis of Chalmers University of Technology, Göteborg, Sweden, 2001.
[7] P. Miron, C. Bérat, V. Sabelnikov, Effect of blowing rate on the film cooling coverage on a multi-holed plate: application on combustor walls, in: Eighth International Conference on Advanced Computational Methods in Heat Transfer, Lisbon, Portugal, 2004.
[8] R.K. Hanson, J.M. Seitzman, P.H. Paul, Planar laser-fluorescence imaging of combustion gases, Applied Physics B 50 (1990) 441–454.
[9] D.G. Bogard, K.A. Thole, Gas turbine film cooling, Journal of Propulsion and Power 22 (2006) 249–270.
[10] J.N. Shadid, E.R.G. Eckert, The mass transfer analogy to heat transfer in fluids with temperature-dependent properties, ASME Journal of Turbomachinery 113 (1991) 27–33.
[11] S. Mendez, F. Nicoud, Adiabatic homogeneous model for flow around a multiperforated plate, AIAA Journal 46 (10) (2008) 2623–2633.